

Robust Frequency Regulation Capacity Scheduling Algorithm for Electric Vehicles

Enxin Yao, *Student Member, IEEE*, Vincent W.S. Wong, *Fellow, IEEE*,
and Robert Schober, *Fellow, IEEE*

Abstract—Electric vehicles (EVs) have the potential to provide frequency regulation service to an independent system operator (ISO) by changing their real-time charging or discharging power according to an automatic generation control (AGC) signal. Recently, the Federal Energy Regulatory Commission has issued Order 755 to ISOs to introduce a performance-based compensation scheme in the frequency regulation market. The goal is to provide economic incentives for fast ramping resources such as EVs to participate in the market. In this paper, we model the EV frequency regulation service under the performance-based compensation scheme. Thereby, a robust optimization framework is adopted for the formulation of a frequency regulation capacity scheduling problem. Our problem formulation takes into account the performance-based compensation scheme, the random AGC signal, and the dynamic arrival and departure times of the EVs. We propose an efficient algorithm to solve the formulated problem. Simulation results show that the proposed algorithm improves the revenue under the performance-based compensation scheme compared to a benchmark algorithm.

Keywords—Electric vehicles, frequency regulation, robust optimization, scheduling algorithm.

I. INTRODUCTION

Electric vehicles (EVs) are among the potential candidates to replace combustion engine vehicles in an effort to reduce the emission of CO_2 and other greenhouse gases. EVs have the potential to provide additional services besides driving. For example, when EVs are connected with the power grid, they can be coordinated to change their real-time charging or discharging power and provide *frequency regulation* service to an independent system operator (ISO), such as the California ISO (CAISO). Frequency regulation service helps ISOs to keep the utility frequency around the nominal value (e.g., 50 Hertz or 60 Hertz) by compensating short term mismatches between generation and load. The pilot projects in [1], [2] show that EVs are able to provide frequency regulation service by following an *automatic generation control* (AGC) signal issued by the ISO. Fast ramping resources such as EVs can reduce the overall frequency regulation capacity requirement for ISOs and lead to lower costs for the consumers [3].

Most of the EV frequency regulation literature falls into one of two categories. The works in the first category, e.g., [4]–[7], propose control algorithms for EVs to provide frequency

regulation service autonomously, whereby EVs sense the utility frequency deviation locally. In contrast, a market-based EV frequency regulation service is considered by the papers in the second category, e.g., [8]–[19]. In this case, the ISO purchases hourly regulation capacities in a frequency regulation market and the participating EVs are obliged to change their real-time charging or discharging power according to an AGC signal. An *aggregator* is typically used to serve as an agent between the ISO and the fleet of EVs. In [8]–[10], algorithms for the aggregator to distribute regulation tasks among EVs are proposed. The interaction between the aggregator and EVs is analyzed in [11]. Several algorithms for the aggregator and EVs to schedule the hourly regulation capacities are reported in [12]–[16]. The algorithm proposed in [12] aims to maximize the revenue while satisfying the charging demand requirement. In [13], a framework for unidirectional EV frequency regulation service is proposed where the EVs track the AGC signal by changing their real-time charging power around a baseline. Unidirectional EV frequency regulation is of practical interest as EV owners may not allow the discharging of their EVs because of the negative impact of frequent discharging on the lifetime of batteries. Moreover, EV manufacturers may not honor the warranty for EV batteries, if the battery is frequently discharged to provide frequency regulation service. Furthermore, the algorithm proposed in [14] takes into account the market rules for the wholesale electricity energy market and the ancillary service market. In [15], a stochastic algorithm is developed by considering the randomness of the prices and the AGC signal. A bidding algorithm for the aggregator to participate in the day-ahead market based on stochastic optimization is proposed in [17]. In [18], a multi-layered control algorithm to set the real-time charging rate of the EVs based on their charging priority is reported.

We note that the authors of [8]–[18] consider capacity-based frequency regulation compensation, where the revenue depends on the hourly regulation capacity. However, the Federal Energy Regulatory Commission (FERC) issued Order 755 [20] in Oct. 2011, which requires ISOs to introduce a performance-based compensation scheme in their frequency regulation market. Under this scheme, the compensation for the frequency regulation service depends on the performance of the EVs in following the AGC signal, i.e., whether the EVs track the AGC signal closely or not. The goal is to encourage the usage of fast ramping resources (e.g., EVs, battery systems, flywheels) in the frequency regulation market. Performance-based compensation schemes have been implemented by most ISOs in the United States, e.g., the Pennsylvania Jersey

Manuscript was received on Feb. 28, 2015, revised on July 7, 2015, Oct. 20, 2015, and Jan. 27, 2016, and accepted on Feb. 6, 2016. This work is supported by the Natural Sciences and Engineering Research Council of Canada (NSERC) under Strategic Project Grant (STPGP 447607-13). E. Yao, V.W.S. Wong, and R. Schober are with the Department of Electrical and Computer Engineering, The University of British Columbia, Vancouver, BC, Canada, V6T 1Z4, email: {enxin Yao, vincentw, rschober}@ece.ubc.ca.

Maryland Interconnection (PJM), CAISO, New York ISO, and Midcontinent ISO. They provide economic incentives to encourage the ramping resources to respond to the AGC signal quickly, accurately, and reliably.

One method for improving the revenue of the EV frequency regulation service under the performance-based compensation scheme is to ensure that the EVs follow the AGC signal reliably. However, an EV cannot follow the AGC signal to charge if it is fully charged and it cannot discharge if its battery is depleted of energy. On the other hand, the batteries of the EVs may either get fully charged or depleted unexpectedly when the EVs follow the random AGC signal all the time. References [21], [22] show that a filtered AGC signal can improve the reliability of the EVs in following the AGC signal but can be used only by those ISOs (e.g., PJM) which require that the regulation up capacity be equal to the regulation down capacity. Since the performance-based compensation scheme has been implemented by the ISOs, it is desirable to design new algorithms which improve the revenue of the EV frequency regulation service for this new compensation scheme. The main contributions of this paper can be summarized as follows:

- We model the EV frequency regulation service under the performance-based compensation scheme. This new compensation scheme has been implemented recently by the ISOs in the United States but its significance on the EV frequency regulation service has not yet been studied.
- We develop a new problem formulation for scheduling the regulation capacity of the EVs. Thereby, the revenue under the performance-based compensation scheme is introduced in the objective function. Moreover, we use a robust optimization framework in the formulation to encourage the EVs to follow the uncertain AGC signal reliably most of the time. An efficient algorithm is developed to solve the formulated problem.
- We evaluate the performance of the proposed algorithm and the EV frequency regulation service by simulations. To this end, real AGC signal and prices from PJM are used in our simulations. The results show that the proposed algorithm can improve the revenue of the EV frequency regulation service by around 10% compared to a benchmark algorithm under the performance-based compensation scheme.

We note that our work is different from [15] and [16]. First, we consider a performance-based compensation scheme whereas [15] and [16] focus on capacity-based compensation. Second, we use robust optimization to account for the uncertainty in the AGC signal. The proposed robust optimization algorithm does not require an hourly dynamic update of the capacity. On the other hand, the authors of [15] and [16] use Markov decision process and stochastic dynamic programming to model an aggregator which dynamically updates its capacity at the beginning of each hour. The ISOs in the United States have different market rules and may or may not allow an hourly dynamic update of the capacity [23], [24].

This paper is organized as follows. The system model is introduced in Section II. In Section III, we formulate the

TABLE I
LIST OF NOTATIONS AND VARIABLES USED IN THIS PAPER.

\mathcal{M}	Set of EVs
\mathcal{H}	Set of hours
\mathcal{T}	Set of time slots in one hour
i	Index of an EV in set \mathcal{M}
h	Index of an hour in set \mathcal{H}
t	Index of a time slot in set \mathcal{T}
$x_i(h)$	Baseline charging power of EV i at hour h
$v_i^u(h)$	Regulation up capacity of EV i at hour h
$v_i^d(h)$	Regulation down capacity of EV i at hour h
$q(h, t)$	AGC signal in time slot t at hour h
$f^u(h)$	Regulation up component of AGC signal at hour h
$f^d(h)$	Regulation down component of AGC signal at hour h
$e_i(h)$	Charged energy of EV i at hour h
$m^u(h)$	Summation of absolute changes of the AGC signal for regulation up at hour h
$m^d(h)$	Summation of absolute changes of the AGC signal for regulation down at hour h
$p^e(h)$	Price of charged energy at hour h
$p^u(h)$	Price of regulation up capacity at hour h
$p^d(h)$	Price of regulation down capacity at hour h
$p^c(h)$	Price of following the AGC signal at hour h
E_i^{\max}	Maximum hourly charged energy of EV i
E_i^{\min}	Minimum hourly charged energy of EV i
$f^{u, \max}$	Maximum value of $f^u(h)$
$f^{d, \max}$	Maximum value of $f^d(h)$
μ^u	Expected value of $f^u(h)$
μ^d	Expected value of $f^d(h)$
λ^u	Expected value of $m^u(h)$
λ^d	Expected value of $m^d(h)$
a_i	Arrival time of EV i
d_i	Departure time of EV i
ψ_i	Demand of charging energy of EV i
η	Parameter to adjust the level of robustness
$s_i(h)$	SOC of EV i at hour h
\mathcal{S}	Set of selected hours when the AGC signal takes worst case values
$ \mathcal{S} $	Cardinality of set \mathcal{S}
Δ	Positive arbitrarily large constant
α	Parameter to indicate whether the ISO has separate regulation up and regulation down markets
τ	Arbitrary hour in set $\{1, \dots, h\}$
$w(\tau)$	Auxiliary variable which takes value in $[0, 1]$
$y(\tau), z$	Auxiliary dual variables in problem (14)
p^b	Price of the battery in EVs
l	Life cycle of the battery
θ	Temperature
$\delta(\theta, s_i(h))$	Severity factor map of the battery degradation cost
$\epsilon_{1,i}(h)$	Auxiliary variable to replace $[x_i(h)]^-$
$\epsilon_{2,i}(h)$	Auxiliary variable to replace $[x_i(h) - v_i^u(h)]^-$
\mathcal{K}	Set of scenarios
ω_k	k th scenario ($k \in \mathcal{K}$) for the arrival and departure times
$\mathcal{P}(\omega_k)$	Probability of scenario ω_k
\mathcal{P}_i	Probability that EV i follows the AGC signal

frequency regulation capacity scheduling problem and develop an efficient algorithm. Numerical results are given in Section IV. The paper is concluded in Section V. For convenience, the notations used in this paper are provided in Table I.

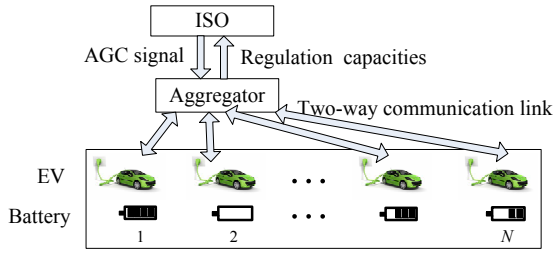


Fig. 1. The EVs provide frequency regulation service by following an AGC signal issued by the ISO. The AGC signal is generated by the ISO in real-time and is random.

II. SYSTEM MODEL

An EV frequency regulation scheme is illustrated in Fig. 1. An aggregator coordinates EVs to provide frequency regulation service to the ISO. First, the aggregator aggregates the hourly frequency regulation capacities of the EVs. The ISO purchases the capacities and the aggregator enters into a contract with the ISO to provide frequency regulation service. Next, during the operation period, the aggregator retrieves the AGC signal issued by the ISO every few seconds (e.g., every 2-6 seconds, depending on the ISO's requirements) and broadcasts the AGC signal to the EVs. The EVs are obliged to provide frequency regulation service by changing their real-time charging or discharging power based on the AGC signal. The information exchange between ISO, aggregator, and EVs is enabled by a two-way communication infrastructure.

We denote the operation hours by $\mathcal{H} = \{1, \dots, H\}$ and the set of EVs by $\mathcal{M} = \{1, \dots, M\}$. In each hour $h \in \mathcal{H}$, EV $i \in \mathcal{M}$ has a baseline charging power $x_i(h)$, regulation up capacity $v_i^u(h)$, and regulation down capacity $v_i^d(h)$. Our goal is to optimize the values of $x_i(h)$, $v_i^u(h)$, and $v_i^d(h)$ to improve the frequency regulation revenue.

A. Randomness of the AGC Signal

The AGC signal is generated by the ISO according to the real-time mismatch between generation and load in the power grid. The AGC signal is updated in short intervals. We divide one hour into multiple time slots. Each time slot corresponds to the duration of one interval of the AGC signal, i.e., one time slot lasts a few seconds. Let $\mathcal{T} = \{1, \dots, T\}$ denote the set of time slots in one hour. The AGC signal in time slot $t \in \mathcal{T}$ at hour $h \in \mathcal{H}$ is denoted by $q(h, t) \in [-1, 1]$.

The AGC signal indicates the amount by which EV $i \in \mathcal{M}$ should increase or decrease its charging power, compared to the baseline charging power $x_i(h)$. A positive AGC signal (i.e., $q(h, t) > 0$) indicates that the power generation is lower than the load. In this case, EV i provides the regulation up service by multiplying the AGC signal with its regulation up capacity $v_i^u(h)$ and decreasing the charging power accordingly. A negative AGC signal (i.e., $q(h, t) < 0$) indicates that the power generation is higher than the load. EV i provides the regulation down service by multiplying the AGC signal with its regulation down capacity $v_i^d(h)$ and increasing the charging power accordingly. Note that for chargers that comply with the Society of Automotive Engineers (SAE) J1772 standard [26], the charging power can be changed by adjusting the duty cycle of the pulse width modulation in the charger's pilot signal

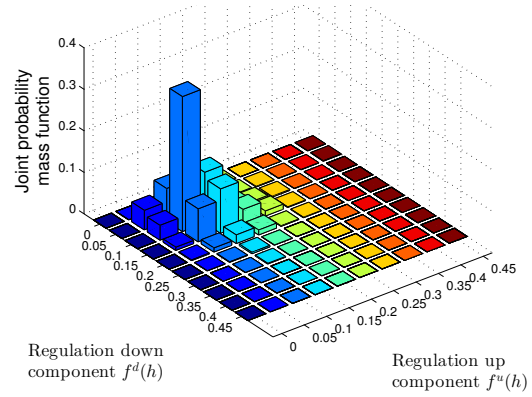


Fig. 2. Joint distribution of the hourly regulation up and regulation down components of an AGC signal. The distribution is obtained by analyzing the AGC signal data records in [25] for 2,208 hours. The figure reveals the randomness of the regulation up and regulation down components.

[8]. In this paper, we assume that the charging power can be continuously adjusted.¹

We analyze the AGC signal on an hourly basis as ISOs typically purchase hourly capacities. We denote the regulation up component and the regulation down component of the AGC signal within hour h by $f^u(h)$ and $f^d(h)$, respectively. We have

$$f^u(h) = \frac{1}{T} \sum_{t \in \mathcal{T}} [q(h, t)]^+, \quad h \in \mathcal{H}, \quad (1)$$

$$f^d(h) = \frac{1}{T} \sum_{t \in \mathcal{T}} [-q(h, t)]^+, \quad h \in \mathcal{H}, \quad (2)$$

where $[x]^+ = \max\{x, 0\}$. Let $e_i(h)$ denote the charged energy for EV i within hour h . Then, $e_i(h)$ can be expressed as

$$\begin{aligned} e_i(h) &= \frac{1}{T} \sum_{t \in \mathcal{T}} (x_i(h) - v_i^u(h) [q(h, t)]^+ + v_i^d(h) [-q(h, t)]^+) \\ &= x_i(h) - v_i^u(h) f^u(h) + v_i^d(h) f^d(h). \end{aligned} \quad (3)$$

The terms $v_i^u(h) f^u(h)$ and $v_i^d(h) f^d(h)$ represent the discharged and charged energy due to following the regulation up and regulation down components of the AGC signal during hour h , respectively. Note that we assume EVs follow the AGC signal in every time slot because EVs are fast ramping resources that have zero lost opportunity cost [21], [24].

The random AGC signal leads to an uncertainty in the charged or discharged energy of the EVs, as shown in (3). Hence, we studied the statistical joint distribution of $f^u(h)$ and $f^d(h)$, i.e., $\mathcal{P}(f^u(h), f^d(h))$, by analyzing the AGC signal data records of PJM [25], for the period from March 1, 2014 to May 31, 2014. The results are shown in Fig. 2 and reveal that $f^u(h)$ and $f^d(h)$ may deviate significantly from their expected values.

¹Some EVs may be equipped with simple chargers which can only be turned on and off. These EVs are still able to provide frequency regulation service and a corresponding dispatching algorithm based on a priority list has been proposed in [8]. If the EV chargers can only be turned on and off, an EV either has a zero baseline charging power when providing regulation down capacity or has a full baseline charging rate when providing regulation up capacity. Hence, $v_i^u(h)$, $v_i^d(h)$, and $x_i(h)$ become integer variables if EV chargers can only be turned on and off. In this case, we would have an additional constraint $x_i(h), v_i^u(h), v_i^d(h) \in \{0, e_i^{\max}\}$, $i \in \mathcal{M}, h \in \mathcal{H}$, where e_i^{\max} is the maximum charging rate of EV i , and an integer programming problem is formulated.

B. Performance-based Frequency Regulation Compensation

The ISO makes two payments under the performance-based frequency regulation compensation scheme. First, the ISO purchases the regulation up and regulation down capacities at hour h at prices $p^u(h)$ and $p^d(h)$, respectively. Second, the ISO makes another payment for EVs that follow the AGC signal (e.g., the regulation market performance clearing price (RMPCP) in PJM). The corresponding performance price is denoted by $p^c(h)$. Let $m^u(h)$ and $m^d(h)$ denote the summation of the absolute changes of the regulation up and regulation down elements of the AGC signal, respectively. We have

$$m^u(h) = \sum_{t \in \mathcal{T}} \left| [q(h, t)]^+ - [q(h, t-1)]^+ \right|, \quad h \in \mathcal{H}, \quad (4)$$

$$m^d(h) = \sum_{t \in \mathcal{T}} \left| [-q(h, t)]^+ - [-q(h, t-1)]^+ \right|, \quad h \in \mathcal{H}, \quad (5)$$

where $|\cdot|$ denotes the absolute value. We assume the communication links between the ISO, aggregator, and EVs are reliable. If EV i follows the AGC signal at hour h , it receives a performance related payment of $p^c(h)(v_i^u(h)m^u(h) + v_i^d(h)m^d(h))$. Let $\mathbf{1}_{i,h}$ denote an indicator function, which is equal to 1 when EV i follows the AGC signal in hour h , and is equal to 0 otherwise. We denote the price for purchasing energy at hour h by $p^e(h)$. The revenue for EV i at hour h is denoted by $r_i(v_i^u(h), v_i^d(h), x_i(h))$, and can be written as

$$\begin{aligned} r_i(v_i^u(h), v_i^d(h), x_i(h)) = & -p^e(h) \left(x_i(h) - v_i^u(h)f^u(h) \right. \\ & \left. + v_i^d(h)f^d(h) \right) + \xi_i \left((p^u(h)v_i^u(h) + p^d(h)v_i^d(h)) \right. \\ & \left. + \mathbf{1}_{i,h}p^c(h) (v_i^u(h)m^u(h) + v_i^d(h)m^d(h)) \right), \quad (6) \end{aligned}$$

where $-p^e(h)(x_i(h) - v_i^u(h)f^u(h) + v_i^d(h)f^d(h))$, $p^u(h)v_i^u(h) + p^d(h)v_i^d(h)$, and $p^c(h)(v_i^u(h)m^u(h) + v_i^d(h)m^d(h))$ represent the cost for the charged energy, payment for the regulation capacity, and the payment for following the AGC signal, respectively. The coefficient $\xi_i \in [0, 1]$ in (6) is referred to as the performance score in [24]. It is determined by the ISO according to the performance of the EVs in following the AGC signal in past hours. If EV i fails to follow the AGC signal at hour h (i.e., $\mathbf{1}_{i,h} = 0$), the ISO will degrade the score in future hours. Note that the ISO takes into account the performance over a long period (e.g., 100 hours in PJM) to calculate the performance score. Hence, it is difficult to explicitly calculate the degradation of the revenue and performance score when EV i fails to follow the AGC signal at hour h . Instead, we aim to attain a performance score close to 1 by ensuring that EVs follow the AGC signal most of the time.

Equation (6) models the essence of the performance-based compensation scheme in [24]. In practice, for the calculation of the performance score, the ISO first compares the trajectory of the EVs' charging power with the AGC signal and uses a correlation coefficient to measure the accuracy of the EVs' frequency regulation service for each hour [24]. The delay of the EVs in responding to the AGC signal is taken into account by the ISO. The performance score is then calculated by the ISO according to the performance of the EVs over the

past hours. In order to have a tractable problem formulation, we model the revenue calculation method in [24] by equation (6), which reflects several important characteristics of the performance-based compensation scheme. First, the ISO uses a performance score as a multiplier for the revenue. The EVs should track the AGC signal quickly, accurately, and reliably to improve the performance score. Second, an additional payment for following the AGC signal is introduced in the performance-based compensation scheme. Third, the payment for following the AGC signal is calculated based on the absolute change of the AGC signal, which is referred to as the mileage of the AGC signal in [24]. Although the ISOs have implemented different market rules under Order 755 issued by the FERC, the above three characteristics are common to all performance-based compensation schemes.

The EVs' limited battery capacity makes it challenging to follow the AGC signal reliably. An EV cannot charge when its battery is fully charged, even if this is mandated by the AGC signal. Similarly, it cannot discharge when its battery is depleted. In the next section, we use a robust optimization framework to obtain the hourly regulation capacities and enable EVs to follow the AGC signal most of the time.

III. PROBLEM FORMULATION

In this section, we formulate an EV frequency regulation capacity scheduling problem based on the robust optimization framework in [27]. The formulated problem aims to select $v_i^u(h)$, $v_i^d(h)$, and $x_i(h)$ in order to maximize the revenue under the performance-based compensation scheme. The uncertain parameters of the AGC signal $f^u(h)$ and $f^d(h)$, $h \in \mathcal{H}$ are considered in the formulated problem to ensure that the EVs follow the AGC signal most of the time. We note that we do not aim to guarantee that EVs always strictly follow the random AGC signal, because such a guarantee may lead to a very conservative solution (i.e., a small regulation capacity) and reduce the revenue of the EVs.

We adopt the robust optimization framework in [27] to formulate our problem. We use this framework because some of the constraints in our problem include multiple uncertain parameters and should be satisfied with a high probability. Note that the framework in [27] is different from most of the other robust optimization frameworks which consider hard constraints (e.g., [28]). A robust optimization framework with hard constraints ensures that the solution is always feasible when the uncertain parameters are within their uncertainty sets. Hard constraints are suitable only if the constraints are highly critical. However, hard constraints are not suitable to our problem because they may result in conservative solutions and reduce the revenue obtained from the EV frequency regulation service. Note that an alternative approach is to use chance constraints in our formulation. We use the framework in [27] instead of chance constraints because the formulated problem can be solved efficiently.

The basic idea of the framework in [27] is that, although a single uncertain parameter sometimes may take its worst case value, it rarely happens that all the parameters take their worst case values simultaneously. Hence, the framework

in [27] introduces a tunable design parameter to adjust the number of uncertain parameters which will take their worst case values simultaneously. With an appropriate selection of the number of parameters assuming worst case values, the probability for the scenarios in practical systems to be worse than the scenarios considered in the formulation is small. In this case, the constraints which include uncertain parameters are satisfied with a high probability. In this paper, we borrow the basic idea of framework in [27] and introduce an integer parameter $\eta \in \{0, 1, \dots, H\}$. Our formulation ensures that the EVs follow an AGC signal where the unknown parameters $f^u(h)$ and $f^d(h)$ take worst case values in at most η hours and take their expected values in the remaining hours.

Let τ represent an arbitrary hour in the set $\mathcal{H}(h) = \{1, \dots, h\}$. We denote $\mathcal{S} \subseteq \mathcal{H}(h)$ as the set of hours when $f^u(\tau)$ and $f^d(\tau)$ take their worst case values. The cardinality of set \mathcal{S} is denoted by $|\mathcal{S}|$. The expected values of $f^u(\tau)$ and $f^d(\tau)$ are denoted by μ^u and μ^d , respectively. The uncertainty sets of $f^u(h)$ and $f^d(h)$ are denoted by $f^u(h) \in [0, f^{u,\max}]$, $f^d(h) \in [0, f^{d,\max}]$. The constants $f^{u,\max}$ and $f^{d,\max}$ denote the maximum values of the regulation up and regulation down components of the AGC signal, respectively. The values of $f^{u,\max}$ and $f^{d,\max}$ can be obtained by analyzing historical AGC signal data (see Section IV). We consider two cases for $f^u(\tau)$ and $f^d(\tau)$. In the first case, $f^u(\tau)$ and $f^d(\tau)$ take worst case values in the set of hours \mathcal{S} to *increase the SOC* of the EVs (i.e., $f^u(\tau) = 0, f^d(\tau) = f^{d,\max}, \tau \in \mathcal{S}$). Let $s_i(0)$ denote the initial SOC of EV i at the beginning of the operation hours. We denote the battery capacity of EV i as B_i . We assume the charging efficiencies of both charger and battery are close to one. For EV $i \in \mathcal{M}$ and hour $h \in \mathcal{H}$, we have the following constraint

$$s_i(0) + \max_{\{\mathcal{S} \subseteq \mathcal{H}(h) \mid |\mathcal{S}| \leq \eta\}} \left(\frac{1}{B_i} \sum_{\tau \in \mathcal{S}} (x_i(\tau) - v_i^u(\tau)0 + v_i^d(\tau)f^{d,\max}) \right) + \frac{1}{B_i} \sum_{\tau \in \mathcal{H}(h) \setminus \mathcal{S}} (x_i(\tau) - v_i^u(\tau)\mu^u + v_i^d(\tau)\mu^d) \leq s^{\max}, \quad (7)$$

where s^{\max} is the maximum SOC of the EV battery (e.g., $s^{\max} = 1$). $\{\mathcal{S} \subseteq \mathcal{H}(h) \mid |\mathcal{S}| \leq \eta\}$ are all subsets of $\mathcal{H}(h)$ where the number of elements is at most η . In the selected hours $\tau \in \mathcal{S}$, the unknown parameters $f^u(\tau)$ and $f^d(\tau)$ take worst case values (i.e., $f^u(\tau) = 0, f^d(\tau) = f^{d,\max}$) to increase the SOC of EV i , see the first term following the max in (7). In the remaining hours (i.e., $\tau \in \mathcal{H}(h) \setminus \mathcal{S}$), $f^u(\tau)$ and $f^d(\tau)$ take the expected values, see the last term on the left hand side of (7). Constraint (7) can be equivalently rewritten as

$$s_i(0) + \max_{\{\mathcal{S} \subseteq \mathcal{H}(h) \mid |\mathcal{S}| \leq \eta\}} \left(\left(\frac{1}{B_i} \sum_{\tau \in \mathcal{S}} (x_i(\tau) + v_i^d(\tau)f^{d,\max}) - \frac{1}{B_i} \sum_{\tau \in \mathcal{S}} (x_i(\tau) - v_i^u(\tau)\mu^u + v_i^d(\tau)\mu^d) \right) + \left(\frac{1}{B_i} \sum_{\tau \in \mathcal{S}} (x_i(\tau) - v_i^u(\tau)\mu^u + v_i^d(\tau)\mu^d) + \frac{1}{B_i} \sum_{\tau \in \mathcal{H}(h) \setminus \mathcal{S}} (x_i(\tau) - v_i^u(\tau)\mu^u + v_i^d(\tau)\mu^d) \right) \right) \leq s^{\max}. \quad (8)$$

Constraint (8) is equivalent to (7) as we remove and then add the same components in the second and third lines. Constraint (8) can be simplified as

$$s_i(0) + \max_{\{\mathcal{S} \subseteq \mathcal{H}(h) \mid |\mathcal{S}| \leq \eta\}} \left(\frac{1}{B_i} \sum_{\tau \in \mathcal{S}} v_i^u(\tau)\mu^u + v_i^d(\tau)(f^{d,\max} - \mu^d) \right) + \frac{1}{B_i} \sum_{\tau \in \mathcal{H}(h)} (x_i(\tau) - v_i^u(\tau)\mu^u + v_i^d(\tau)\mu^d) \leq s^{\max}. \quad (9)$$

We replace the max operator in (9) using $\max g(x) = -\min(-g(x))$, where $g(x)$ denotes an arbitrary function, and obtain

$$s_i(0) - \frac{1}{B_i} \min_{\{\mathcal{S} \subseteq \mathcal{H}(h) \mid |\mathcal{S}| \leq \eta\}} \left(\sum_{\tau \in \mathcal{S}} -v_i^u(\tau)\mu^u + v_i^d(\tau)(\mu^d - f^{d,\max}) \right) + \frac{1}{B_i} \sum_{\tau \in \mathcal{H}(h)} (x_i(\tau) - v_i^u(\tau)\mu^u + v_i^d(\tau)\mu^d) \leq s^{\max}. \quad (10)$$

Constraint (10) is equivalent to (7) as shown in (8) and (9).

We now consider the second case when the unknown parameters take worst case values to *reduce the SOC* of the EVs (i.e., $f^u(\tau) = f^{u,\max}, f^d(\tau) = 0, \tau \in \mathcal{S}$). For EV $i \in \mathcal{M}$ and hour $h \in \mathcal{H}$, the following constraint keeps the SOC above a minimum

$$s_i(0) + \frac{1}{B_i} \min_{\{\mathcal{S} \subseteq \mathcal{H}(h) \mid |\mathcal{S}| \leq \eta\}} \sum_{\tau \in \mathcal{S}} (v_i^u(\tau)(\mu^u - f^{u,\max}) - v_i^d(\tau)\mu^d) + \frac{1}{B_i} \sum_{\tau \in \mathcal{H}(h)} (x_i(\tau) - v_i^u(\tau)\mu^u + v_i^d(\tau)\mu^d) \geq s^{\min}, \quad (11)$$

where s^{\min} is the minimum SOC of the EV battery (e.g., $s^{\min} = 0$). Constraints (10) and (11) confine the SOC of EV i to be within $[s^{\min}, s^{\max}]$ at hour h . In this paper, we use constraints (10) and (11) to enable the EVs to follow the AGC signal most of the time.

EVs can provide frequency regulation service in two modes, depending on whether discharging is allowed or not. If discharging is allowed, then there is an additional cost of battery degradation. In [29], a framework is proposed to estimate the battery degradation cost using a severity factor map. The severity factor map is a function which maps the temperature and the SOC to a battery degradation factor. Let $\delta(\theta, s_i(h))$ denote the battery degradation factor, where θ is the temperature and $s_i(h)$ is the SOC of EV i at hour h . In [30], the values of the battery degradation factor $\delta(\theta, s_i(h))$ are provided for lithium-ion batteries, which are typically used in EVs. We denote the price of the batteries in the EVs by p^b . The unit of p^b is \$ per kW. The life cycle of the batteries is denoted by l . Furthermore, let a_i , d_i , and ψ_i denote the arrival time, departure time, and charging demand requirement of EV i , respectively. We denote the expected values of the summation of the absolute changes of the regulation up and regulation down components $m^u(h)$ and $m^d(h)$ in (4) and (5) by λ^u and λ^d , respectively. The values of λ^u and λ^d can be obtained based on (4) and (5), and the historical records of the AGC signal. We can formulate an EV frequency regulation capacity scheduling problem as follows:

$$\begin{aligned} & \text{maximize} \sum_{h \in \mathcal{H}} \sum_{i \in \mathcal{M}} \left(\mathbb{E} [p^u(h)] v_i^u(h) + \mathbb{E} [p^d(h)] v_i^d(h) \right. \\ & \left. v_i^u(h), v_i^d(h), \mathbb{E} [p^c(h)] (v_i^u(h) \lambda^u + v_i^d(h) \lambda^d) \right. \\ & \left. x_i(h), i \in \mathcal{M}, + \mathbb{E} [p^e(h)] (x_i(h) - v_i^u(h) \mu^u + v_i^d(h) \mu^d) \right. \\ & \left. - \frac{p^b}{\Gamma} \delta(\theta, s_i(h)) ([x_i(h)]^- + \mu^u [x_i(h) - v_i^u(h)]^-) \right) \end{aligned} \quad (12a)$$

$$\text{subject to } x_i(h) + v_i^d(h) \leq E_i^{\max}, \quad i \in \mathcal{M}, h \in \mathcal{H}, \quad (12b)$$

$$x_i(h) - v_i^u(h) \geq E_i^{\min}, \quad i \in \mathcal{M}, h \in \mathcal{H}, \quad (12c)$$

$$v_i^u(h), v_i^d(h) \geq 0, \quad i \in \mathcal{M}, h \in \mathcal{H}, \quad (12d)$$

$$v_i^u(h) - \alpha \Delta \leq v_i^d(h) \leq v_i^u(h) + \alpha \Delta, \quad i \in \mathcal{M}, \\ h \in \mathcal{H}, \quad (12e)$$

$$- \Delta \mathbf{1}_{a_i \leq h \leq d_i} \leq x_i(h) \leq \Delta \mathbf{1}_{a_i \leq h \leq d_i}, \\ i \in \mathcal{M}, h \in \mathcal{H}, \quad (12f)$$

$$- \Delta \mathbf{1}_{a_i \leq h \leq d_i} \leq v_i^u(h) \leq \Delta \mathbf{1}_{a_i \leq h \leq d_i}, \\ i \in \mathcal{M}, h \in \mathcal{H}, \quad (12g)$$

$$- \Delta \mathbf{1}_{a_i \leq h \leq d_i} \leq v_i^d(h) \leq \Delta \mathbf{1}_{a_i \leq h \leq d_i}, \\ i \in \mathcal{M}, h \in \mathcal{H}, \quad (12h)$$

$$\sum_{\tau=a_i}^{d_i} (x_i(\tau) - v_i^u(\tau) \mu^u + v_i^d(\tau) \mu^d) \geq \psi_i, \\ i \in \mathcal{M}, \quad (12i)$$

constraints (10) and (11),

where $[x_i(h)]^-$ denotes $\max\{-x_i(h), 0\}$ and the term $\frac{p^b}{\Gamma} \delta(\theta, s_i(h)) ([x_i(h)]^- + \mu^u [x_i(h) - v_i^u(h)]^-)$ is the battery degradation cost. $[x_i(h)]^-$ and $\mu^u [x_i(h) - v_i^u(h)]^-$ are used to model the amount of the discharged energy due to a negative baseline charging power $x_i(h)$ and the regulation up service, respectively. Parameter Δ is an arbitrarily large constant, e.g., 10^{10} . $\alpha \in \{0, 1\}$ in (12e) specifies whether the ISO has separate regulation up and regulation down markets ($\alpha = 1$) or requires the regulation up capacity to match the regulation down capacity ($\alpha = 0$). On the other hand, $\mathbb{E} [p^u(h)]$, $\mathbb{E} [p^d(h)]$, $\mathbb{E} [p^c(h)]$, and $\mathbb{E} [p^e(h)]$ in (12a) denote the expected prices for regulation up capacity, regulation down capacity, following the AGC signal, and the charged energy at hour h , respectively.

Objective function (12a) represents an upper bound on the expected aggregate revenue of the EVs. An upper bound is considered because using (6) as the objective function leads to an intractable problem. Note that performance score ξ_i in (6) can be a non-convex function with respect to the capacity. The gap between the upper bound and the expected revenue is obtained by subtracting (6) from (12a) and can be rewritten as $\sum_{h \in \mathcal{H}} \sum_{i \in \mathcal{M}} \left((1 - \xi_i) (\mathbb{E} [p^u(h)] v_i^u(h) + \mathbb{E} [p^d(h)] v_i^d(h)) + (1 - (\xi_i \mathcal{P}(\mathbf{1}_{i,h}))) \mathbb{E} [p^c(h)] (v_i^u(h) \lambda^u + v_i^d(h) \lambda^d) \right)$, where $\mathcal{P}(\mathbf{1}_{i,h})$ represents the probability of $\mathbf{1}_{i,h} = 1$. The gap approaches zero as $\xi_i \rightarrow 1$ and $\mathcal{P}(\mathbf{1}_{i,h}) \rightarrow 1$. In this paper, we aim to ensure $\mathbf{1}_{i,h} = 1$ most of the time using constraints (10) and (11).

Constraints (12b) and (12c) guarantee that the real-time charging power in hour h is within the maximum E_i^{\max} and minimum E_i^{\min} hourly charged energy of EV i . E_i^{\min} is 0 if the EV does not allow discharging. Otherwise, E_i^{\min}

can be negative. With current battery technology, EV owners may not allow discharging of their EVs because this may degrade the battery lifetime. However, in the future, as battery technology evolves and improves, we expect negative E_i^{\min} to become a viable option. Constraint (12d) ensures that the frequency regulation capacities have non-negative values. Constraint (12e) reflects the characteristics of two types of frequency regulation markets. Some ISOs (e.g., PJM, New York ISO) require the frequency regulation service provider to provide the same capacities for regulation up and regulation down services. In this case, $\alpha = 0$, i.e., constraint (12e) can be rewritten as $v_i^u(h) = v_i^d(h)$. On the other hand, some other ISOs (e.g., CAISO, ERCOT) have separate regulation up and regulation down markets. In this case, $\alpha = 1$, i.e., constraint (12e) is always satisfied as Δ is very large. Constraints (12f) (12g), (12h), and (12i) model the different charging periods and demands of EVs. Constraints (12f), (12g), and (12h) ensure that the EVs provide the regulation capacity only when the EVs are connected with the power grid. Note that when $h \in [a_i, d_i]$, constraints (12f), (12g), and (12h) are always satisfied. Otherwise, when $h \notin [a_i, d_i]$, constraints (12f), (12g), and (12h) confine $x_i(h)$, $v_i^u(h)$, and $v_i^d(h)$ to 0. On the other hand, constraint (12i) ensures that the EVs charge sufficient energy before their departure.

Market prices $p^u(h)$, $p^d(h)$, $p^c(h)$, and $p^e(h)$ are unknown parameters. Although including the price uncertainty in the model can make the problem formulation more complete and may further improve the revenue, it may also make the formulation even more complicated. In this paper, we focus on improving the ability of EVs to follow the AGC signal under the uncertainty in the signal. The unknown prices also lead to uncertainty in the revenue but may not prevent the EVs from following the AGC signal. Hence, our model considers the expected values of the prices to reduce the computational complexity. Suboptimal solutions may result if the real values of the prices deviate significantly from their expected values.

A. Duality-based Problem Transformation

Problem (12) is a non-convex problem because constraints (10) and (11) include combinatorial optimization components. We first analyze constraint (10), which includes the combinatorial optimization component

$$\min_{\{S \subseteq \mathcal{H}(h) \mid |S| \leq \eta\}} \sum_{\tau \in S} (-v_i^u(\tau) \mu^u + v_i^d(\tau) (\mu^d - f^{d,\max})).$$

This component can be rewritten as follows [27]

$$\text{minimize} \sum_{w(\tau), \tau \in \mathcal{H}(h)} w(\tau) \left(-v_i^u(\tau) \mu^u + v_i^d(\tau) (\mu^d - f^{d,\max}) \right) \quad (13a)$$

$$\text{subject to } 0 \leq w(\tau) \leq 1, \quad \tau \in \mathcal{H}(h), \quad (13b)$$

$$\sum_{\tau \in \mathcal{H}(h)} w(\tau) \leq \eta, \quad (13c)$$

where $w(\tau)$, $\tau \in \mathcal{H}(h)$, are the variables. Note that the optimal value of problem (13) is equal to the summation of the η smallest values of $(-v_i^u(\tau) \mu^u + v_i^d(\tau) (\mu^d - f^{d,\max}))$ over hours $\tau \in \mathcal{H}(h)$, which is equivalent to the component

$$\min_{\{S \subseteq \mathcal{H}(h) \mid |S| \leq \eta\}} \sum_{\tau \in S} (-v_i^u(\tau) \mu^u + v_i^d(\tau) (\mu^d - f^{d,\max})).$$

Problem (13) is a linear program as it optimizes variables $w(\tau)$. Furthermore, problem (13) is both feasible (e.g., $w(\tau)=0, \tau \in \mathcal{H}(h)$) and bounded ($\sum_{\tau \in \mathcal{H}(h)} \min\{-v_i^u(\tau)\mu^u + v_i^d(\tau)(\mu^d - f^{d,\max}), 0\}$ is a lower bound of the objective function). From the strong duality theorem, the optimal values of problem (13) and its dual problem are the same. The dual problem of (13) can be written as

$$\begin{aligned} & \underset{y(\tau), \tau \in \mathcal{H}(h), z}{\text{maximize}} && -z\eta - \sum_{\tau \in \mathcal{H}(h)} y(\tau) \end{aligned} \quad (14a)$$

$$\begin{aligned} & \text{subject to} && y(\tau) + z \geq v_i^u(\tau)\mu^u - v_i^d(\tau)(\mu^d - f^{d,\max}), \\ & && \tau \in \mathcal{H}(h), \end{aligned} \quad (14b)$$

$$y(\tau), z \geq 0, \quad \tau \in \mathcal{H}(h), \quad (14c)$$

where $y(\tau)$ and z are the dual variables for constraints (13b) and (13c), respectively.

Problem (14) can be used to transform the combinatorial optimization components in constraints (10) and (11). For constraint (10), we replace the component $\min_{\{S \subseteq \mathcal{H}(h) \mid |S| \leq \eta\}} \sum_{\tau \in S} (-v_i^u(\tau)\mu^u + v_i^d(\tau)(\mu^d - f^{d,\max}))$ with the objective function in problem (14) and add all constraints in (14) to problem (12). We use a similar approach to convert constraint (11) in three steps. First, we convert the combinatorial optimization component in constraint (11) into a linear program by substituting $-v_i^u(\tau)\mu^u + v_i^d(\tau)(\mu^d - f^{d,\max})$ in problem (13) with $v_i^u(\tau)(\mu^u - f^{u,\max}) - v_i^d(\tau)\mu^d$. Then, we convert the linear program obtained in the first step into its dual problem. Finally, we substitute the combinatorial optimization component in constraint (11) with the objective function of the dual problem obtained in the second step and add the constraints of the dual problem to problem (12). This leads to the following equivalent problem

$$\begin{aligned} & \underset{\substack{v_i^u(h), v_i^d(h), x_i(h), \\ z_{1,i}(h), z_{2,i}(h), \\ y_{1,i}(h, \tau), y_{2,i}(h, \tau) \\ i \in \mathcal{M}, \tau \in \mathcal{H}(h), \\ h \in \mathcal{H}}}{\text{maximize}} && \sum_{h \in \mathcal{H}} \sum_{i \in \mathcal{M}} \left(\mathbb{E}[p^u(h)] v_i^u(h) + \mathbb{E}[p^d(h)] v_i^d(h) \right. \\ && \left. + \mathbb{E}[p^c(h)] (v_i^u(h)\lambda^u + v_i^d(h)\lambda^d) \right. \\ && \left. - \mathbb{E}[p^e(h)] (x_i(h) - v_i^u(h)\mu^u + v_i^d(h)\mu^d) \right. \\ && \left. - \frac{p_i^b}{T} \delta(\theta, s_i(h)) ([x_i(h)]^- + \mu^u [x_i(h) - v_i^u(h)]^-) \right) \end{aligned} \quad (15a)$$

$$\begin{aligned} & \text{subject to} && s_i(0) + \frac{1}{B_i} \sum_{\tau \in \mathcal{H}(h)} (x_i(\tau) - v_i^u(\tau)\mu^u + v_i^d(\tau)\mu^d) \\ & && + \frac{1}{B_i} (z_{1,i}(h)\eta + \sum_{\tau \in \mathcal{H}(h)} y_{1,i}(h, \tau)) \leq s^{\max}, \\ & && i \in \mathcal{M}, h \in \mathcal{H}, \end{aligned} \quad (15b)$$

$$\begin{aligned} & z_{1,i}(h) + y_{1,i}(h, \tau) \geq v_i^u(\tau)\mu^u - v_i^d(\tau)(\mu^d \\ & - f^{d,\max}), i \in \mathcal{M}, \tau \in \mathcal{H}(h), h \in \mathcal{H}, \end{aligned} \quad (15c)$$

$$\begin{aligned} & s_i(0) + \frac{1}{B_i} \sum_{\tau \in \mathcal{H}(h)} (x_i(\tau) - v_i^u(\tau)\mu^u + v_i^d(\tau)\mu^d) \\ & - \frac{1}{B_i} (z_{2,i}(h)\eta + \sum_{\tau \in \mathcal{H}(h)} y_{2,i}(h, \tau)) \geq s^{\min}, \\ & i \in \mathcal{M}, h \in \mathcal{H}, \end{aligned} \quad (15d)$$

$$\begin{aligned} & z_{2,i}(h) + y_{2,i}(h, \tau) \geq v_i^u(\tau)(f^{u,\max} - \mu^u) \\ & + v_i^d(\tau)\mu^d, i \in \mathcal{M}, \tau \in \mathcal{H}(h), h \in \mathcal{H}, \end{aligned} \quad (15e)$$

$$\begin{aligned} & z_{1,i}(h), z_{2,i}(h), y_{1,i}(h, \tau), y_{2,i}(h, \tau) \geq 0, i \in \mathcal{M}, \\ & \tau \in \mathcal{H}(h), h \in \mathcal{H}, \end{aligned} \quad (15f)$$

constraints (12b)–(12i),

where $(z_{1,i}(h), y_{1,i}(h, \tau))$ and $(z_{2,i}(h), y_{2,i}(h, \tau))$ are dual variables corresponding to the combinatorial optimization components in constraints (10) and (11), respectively. Linear constraints (15b) and (15d) replace constraints (10) and (11) by substituting the involved combinatorial optimization problems with the corresponding linear dual problems. Constraints (15c), (15e), and (15f) are obtained from the constraints in the dual problems. However, the objective function (15a) contains a battery degradation cost $-\frac{p_i^b}{T} \delta(\theta, s_i(h)) ([x_i(h)]^- + \mu^u [x_i(h) - v_i^u(h)]^-)$, which makes problem (15) difficult to solve. Note that the values of $\delta(\theta, s_i(h))$ can be measured experimentally and be recorded in a table [30]. To the best of our knowledge, there is no closed-form expression for the calculation of $\delta(\theta, s_i(h))$ from θ and $s_i(h)$. In order to make problem (15) tractable, we introduce a parameter \bar{s}_i as the expected SOC during the charging period of EV i and auxiliary parameters $\epsilon_{1,i}(h), \epsilon_{2,i}(h), i \in \mathcal{M}, h \in \mathcal{H}$. Then, we rewrite problem (15) as follows:

$$\begin{aligned} & \underset{\substack{v_i^u(h), v_i^d(h), x_i(h), \\ z_{1,i}(h), z_{2,i}(h), \\ y_{1,i}(h, \tau), y_{2,i}(h, \tau) \\ \epsilon_{1,i}(h), \epsilon_{2,i}(h) \\ i \in \mathcal{M}, \tau \in \mathcal{H}(h), \\ h \in \mathcal{H}}}{\text{maximize}} && \sum_{h \in \mathcal{H}} \sum_{i \in \mathcal{M}} \left(\mathbb{E}[p^u(h)] v_i^u(h) + \mathbb{E}[p^d(h)] v_i^d(h) \right. \\ && \left. + \mathbb{E}[p^c(h)] (v_i^u(h)\lambda^u + v_i^d(h)\lambda^d) \right. \\ && \left. - \mathbb{E}[p^e(h)] (x_i(h) - v_i^u(h)\mu^u + v_i^d(h)\mu^d) \right. \\ && \left. - \frac{p_i^b}{T} \delta(\theta, \bar{s}_i) (\epsilon_{1,i}(h) + \mu^u \epsilon_{2,i}(h)) \right) \end{aligned} \quad (16a)$$

$$\text{subject to} \quad \epsilon_{1,i}(h), \epsilon_{2,i}(h) \geq 0, i \in \mathcal{M}, h \in \mathcal{H}, \quad (16b)$$

$$\epsilon_{1,i}(h) \geq -x_i(h), i \in \mathcal{M}, h \in \mathcal{H}, \quad (16c)$$

$$\epsilon_{2,i}(h) \geq -x_i(h) + v_i^u(h), i \in \mathcal{M}, h \in \mathcal{H}, \quad (16d)$$

constraints (12b)–(12i), (15b)–(15f).

Constraints (16b), (16c), and (16d) ensure that $\epsilon_{1,i}(h) \geq [x_i(h)]^-$ and $\epsilon_{2,i}(h) \geq [x_i(h) - v_i^u(h)]^-$. As the objective function in (16a) is decreasing with respect to $\epsilon_{1,i}(h)$ and $\epsilon_{2,i}(h)$, we have $\epsilon_{1,i}(h) = [x_i(h)]^-$ and $\epsilon_{2,i}(h) = [x_i(h) - v_i^u(h)]^-$ when the objective function is maximized.

With the solution obtained in problem (16), the EVs are able to follow an AGC signal for which parameters $f^u(h)$ and $f^d(h), h \in \mathcal{H}$, take their worst case values in at most η hours and take their expected values in other hours. With an appropriate value of η , the probability that the AGC signal in a practical system is worse than the AGC signal considered in problem (12) is small (see Section III-B). In this case, the constraints in problem (12) are satisfied with a high probability with the AGC signal in a practical system.

B. Probability Bound and Selection of Parameter η

Problem (16) aims to enable the EVs to follow the AGC signal with a high probability. Let \mathcal{P}_i denote the probability that EV i follows the AGC signal. Assume that the values of $f^u(h)$ and $f^d(h)$ in hour h are independent of their values in other hours. According to [27, Theorem 3], a lower bound on

probability \mathcal{P}_i is given by

$$\mathcal{P}_i \geq \frac{1}{d_i - a_i + 1} \sum_{h=a_i}^{d_i} \left(1 - \frac{1}{2^{h-a_i}} \left((1 - \mu_i) \binom{h-a_i}{\lfloor \nu_i \rfloor} + \sum_{l=\lfloor \nu_i \rfloor + 1}^{h-a_i} \binom{h-a_i}{l} \right) \right), \quad (17)$$

where $\nu_i = \frac{\eta + h - a_i}{2}$, $\mu_i = \nu_i - \lfloor \nu_i \rfloor$, and $\lfloor \cdot \rfloor$ denotes the floor function. Equation (17) provides a lower bound such that the probability that EV i follows the AGC signal is not less than the right hand side of (17).

The lower bound on probability \mathcal{P}_i in (17) is tuned by design parameter η . To be specific, increasing η increases the lower bound and enables the EVs to follow the AGC signal more reliably. On the other hand, decreasing η enables the EVs to provide more frequency regulation capacity. The optimal choice of η depends on the characteristics of the AGC signal (especially whether the AGC signal will deviate in the same direction repeatedly in multiple hours), and may vary from one ISO to another. As the statistical characteristics of the AGC signal may not change frequently, a simulation study can be used to select an appropriate value of η , see Fig. 8 in Section IV.

On the other hand, the lower bound on probability \mathcal{P}_i in (17) is helpful for selecting an appropriate value of η . We first select a desired value for \mathcal{P}_i , e.g., 95%. Then, as (17) can be calculated efficiently, we find the largest value of η (denoted by $\hat{\eta}$) for which (17) is satisfied. The appropriate value of η should be selected from $[0, \hat{\eta}]$ because the right hand side of (17) is a lower bound on probability \mathcal{P}_i . We use the above method in our simulations in Section IV.

C. Trajectory of the AGC Signal in Hour h

In this section, we verify that the uncertainty sets of $f^u(h)$ and $f^d(h)$ contain the worst-case trajectories of the AGC signal in hour h . Note that two different AGC signal trajectories in hour h with the same values of $f^u(h)$ and $f^d(h)$ may have different effects on the SOC of the EV battery during hour h . On the other hand, it is difficult to directly model the trajectory as there are a large number of possible trajectories. In this section, we study the AGC signal trajectory on an hourly basis and have the following remark.

Remark 1: For an arbitrary hour h , if an EV is able to follow the AGC signal in the two extreme cases, namely the case when $(f^u(h) = f^{u,\max}, f^d(h) = 0)$, and the case when $(f^u(h) = 0, f^d(h) = f^{d,\max})$, then the EV is able to follow the AGC signal under other possible trajectories within hour h , as long as $f^u(h)$ and $f^d(h)$ are in the ranges of $f^u(h) \in [0, f^{u,\max}]$ and $f^d(h) \in [0, f^{d,\max}]$, respectively.

We first consider two trajectories Ω_1 and Ω_2 of the AGC signal within hour h , for which the battery SOC of an EV has the largest deviation. For the first trajectory Ω_1 , the AGC signal has all the regulation up component $f^{u,\max}$ since the beginning of the hour to a certain time \hat{t}_1 and regulation down component $f^{d,\max}$ since \hat{t}_1 to the end of the hour, c.f. Fig. 3(a). For the second trajectory Ω_2 , the AGC signal has all the

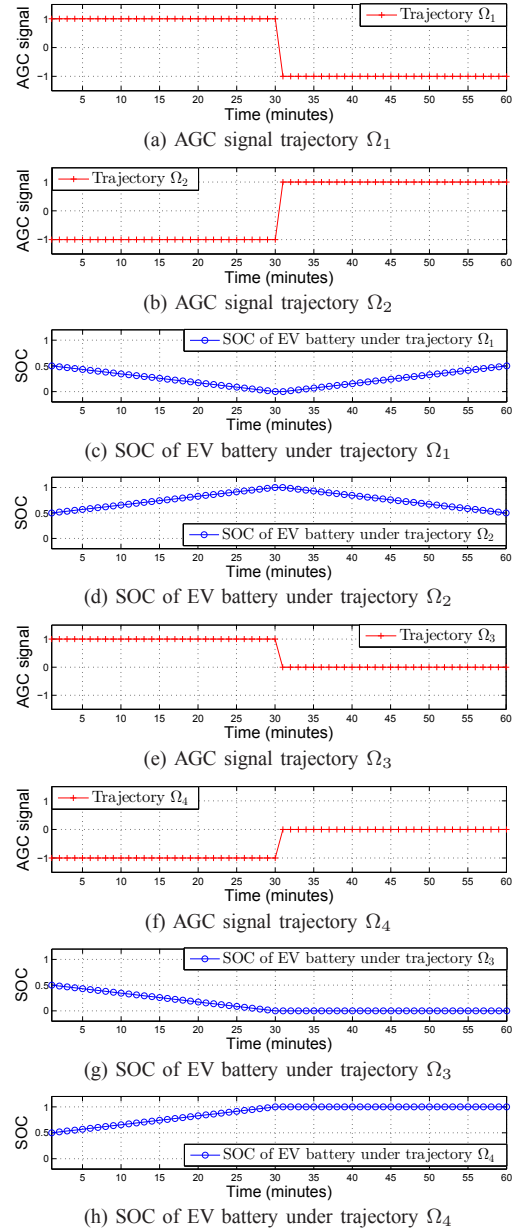


Fig. 3. Different trajectories of the AGC signal and the corresponding SOC of the EV battery. The initial SOC is set to be 0.5.

regulation down component $f^{d,\max}$ since the beginning of the hour to a certain time \hat{t}_2 and the regulation up component since \hat{t}_2 to the end of the hour, c.f. Fig. 3(b). Ω_1 and Ω_2 are the worst case trajectories of the AGC signal in hour h . The battery SOC of an EV has the largest downward and upward deviations under Ω_1 and Ω_2 , c.f. Figs. 3(c) and 3(d).

For trajectory Ω_1 in hour h , the SOC of an EV battery reaches a minimum at \hat{t}_1 , c.f. Fig. 3(c). In our problem formulation, we consider a case when $f^u(h) = f^{u,\max}$ and $f^d(h) = 0$. A possible trajectory Ω_3 of the AGC signal with $f^u(h) = f^{u,\max}$ and $f^d(h) = 0$ is illustrated in Fig. 3(e). The SOC of an EV battery at the end of hour h under trajectory Ω_3 is equivalent to the minimum SOC in hour h under trajectory Ω_1 , c.f. Figs. 3(c) and 3(g). Note that an EV has the largest downward deviation of the battery SOC under trajectory Ω_1 in hour h . If the battery SOC of an EV remains above the

minimum value under trajectory Ω_3 at the end of hour h , the SOC will remain above the minimum value for other trajectories with $f^u(h) \in [0, f^{u,\max}]$ and $f^d(h) \in [0, f^{d,\max}]$. Similarly, for the second trajectory Ω_2 in hour h , we show that the maximum SOC in hour h under Ω_2 is the same as the SOC at the end of hour h in a case when $f^u(h) = 0$ and $f^d(h) = f^{d,\max}$, see Figs. 3(d) and 3(h).

As explained in Remark 1 in the above, for a *single* hour h , the worst case trajectory of the AGC signal in hour h is contained in the uncertainty sets of $f^u(h)$ and $f^d(h)$. On the other hand, note that the EVs need to follow the AGC signal in *multiple* hours. Our problem formulation considers the scenario where parameters $f^u(h)$ and $f^d(h)$, $h \in \mathcal{H}$, of the AGC signal can take their worst case values in a limited number of hours (at most η hours).

D. Stochastic Arrival and Departure of the EVs

In this section, we extend our problem formulation to a case where EVs have stochastic arrival and departure times. In Section III-A, we have assumed that the arrival and departure times are known. In practice, the arrival and departure times of the EVs can be uncertain parameters.

Two issues need to be considered when the EVs have uncertain arrival and departure times. The first issue concerns the entity to perform the scheduling of regulation capacity. When the arrival time is known, the aggregator schedules the regulation capacity in a centralized manner. However, if the arrival time is unknown, the regulation capacity needs to be determined by the EVs independently. Second, if the arrival time is unknown, the EV needs to consider different scenarios. A scenario is a possible realization of the future arrival time, departure time, and charging demand requirement. The scenarios can be generated based on the historical records of the EVs. Let $\omega_k, k \in \mathcal{K}$ denote a scenario where $\mathcal{K} = \{1, \dots, K\}$ is the set of scenarios. The scenarios can be generated based on historical records of EVs arrival and departure times. The probability for scenario ω_k is denoted by $\mathcal{P}(\omega_k)$. We denote the arrival time, departure time, and charging demand requirement of EV i for scenario ω_k by $a_i(\omega_k)$, $d_i(\omega_k)$, and $\psi_i(\omega_k)$ respectively. Let $v_i^u(h, \omega_k)$, $v_i^d(h, \omega_k)$, $x_i(h, \omega_k)$, $z_{1,i}(h, \omega_k)$, $z_{2,i}(h, \omega_k)$, $y_{1,i}(h, \tau, \omega_k)$, $y_{2,i}(h, \tau, \omega_k)$, $\epsilon_{1,i}(h, \omega_k)$, and $\epsilon_{2,i}(h, \omega_k)$ denote the values of $v_i^u(h)$, $v_i^d(h)$, $x_i(h)$, $z_{1,i}(h)$, $z_{2,i}(h)$, $y_{1,i}(h, \tau)$, $y_{2,i}(h, \tau)$, $\epsilon_{1,i}(h)$, and $\epsilon_{2,i}(h)$ under scenario ω_k , respectively. For EV $i \in \mathcal{M}$, the problem to schedule the regulation capacity can be rewritten as

$$\begin{aligned} & \text{maximize} && \sum_{k \in \mathcal{K}} \mathcal{P}(\omega_k) \sum_{h \in \mathcal{H}} \sum_{i \in \mathcal{M}} \left(\mathbb{E} [p^u(h)] v_i^u(h, \omega_k) \right. \\ & v_i^u(h, \omega_k), && + \mathbb{E} [p^d(h)] v_i^d(h, \omega_k) \\ & v_i^d(h, \omega_k), && + \mathbb{E} [p^c(h)] (v_i^u(h, \omega_k) \lambda^u + v_i^d(h, \omega_k) \lambda^d) \\ & x_i(h, \omega_k), && + \mathbb{E} [p^e(h)] (x_i(h, \omega_k) \\ & z_{1,i}(h, \omega_k), && - v_i^u(h, \omega_k) \mu^u + v_i^d(h, \omega_k) \mu^d) \\ & z_{2,i}(h, \omega_k), && - v_i^u(h, \omega_k) \mu^u + v_i^d(h, \omega_k) \mu^d) \\ & y_{1,i}(h, \tau, \omega_k), && - \frac{p^b}{\tau} \delta(\theta, \bar{s}_i) (\epsilon_{1,i}(h, \omega_k) + \mu^u \epsilon_{2,i}(h, \omega_k)) \\ & y_{2,i}(h, \tau, \omega_k), && \\ & \epsilon_{1,i}(h, \omega_k), && \\ & \epsilon_{2,i}(h, \omega_k), && \\ & \tau \in \mathcal{H}(h), && \\ & h \in \mathcal{H} && \end{aligned} \quad (18a)$$

$$\text{subject to} \quad -\Delta \mathbf{1}_{a_i(\omega_k) \leq h \leq d_i(\omega_k)} \leq x_i(h, \omega_k)$$

$$\leq \Delta \mathbf{1}_{a_i(\omega_k) \leq h \leq d_i(\omega_k)}, \quad h \in \mathcal{H}, k \in \mathcal{K}, \quad (18b)$$

$$\begin{aligned} & -\Delta \mathbf{1}_{a_i(\omega_k) \leq h \leq d_i(\omega_k)} \leq v_i^u(h, \omega_k) \\ & \leq \Delta \mathbf{1}_{a_i(\omega_k) \leq h \leq d_i(\omega_k)}, \quad h \in \mathcal{H}, k \in \mathcal{K}, \quad (18c) \end{aligned}$$

$$\begin{aligned} & -\Delta \mathbf{1}_{a_i(\omega_k) \leq h \leq d_i(\omega_k)} \leq v_i^d(h, \omega_k) \\ & \leq \Delta \mathbf{1}_{a_i(\omega_k) \leq h \leq d_i(\omega_k)}, \quad h \in \mathcal{H}, k \in \mathcal{K}, \quad (18d) \end{aligned}$$

$$\begin{aligned} & \sum_{\tau = a_i(\omega_k)}^{d_i(\omega_k)} (x_i(\tau, \omega_k) - v_i^u(\tau, \omega_k) \mu^u + v_i^d(\tau, \omega_k) \mu^d) \\ & \geq \psi_i(\omega_k), \quad k \in \mathcal{K}, \quad (18e) \end{aligned}$$

constraints (12b)–(12e), (15b)–(15f), and

$$(16b)–(16d).$$

Constraints (18b)–(18e) extend constraints (12f)–(12i) under scenario ω_k . Problem (18) can be solved to obtain the scheduling results under different scenarios.

E. Aggregate Capacity in the Day-ahead Market

The aggregator participates in the day-ahead market (DAM) of an ISO to sell the aggregate capacity of the EVs. In this section, we develop a method to determine the amount of regulation capacity submitted in the DAM. We aim to ensure that the EVs can provide the capacity on the next day according to the amount submitted in the DAM. Let $v^u(h)$ and $v^d(h)$ denote the regulation up capacity and regulation down capacity submitted in the DAM, respectively. The aggregator needs to determine control variables $v^u(h)$ and $v^d(h)$ in order to participate in the DAM.

The uncertain aggregate capacity of the EVs can be modeled as normal distributed based on the Lyapunov central limit theorem (CLT) [31]. Note that the Lyapunov CLT does not require the involved random variables to have identical distributions, and hence, it is applicable to the regulation capacity of the EVs. According to the Lyapunov CLT, the aggregate capacities $\sum_{i \in \mathcal{M}} v_i^u(h)$ and $\sum_{i \in \mathcal{M}} v_i^d(h)$ follow normal distributions when the number of EVs is large and both $v_i^u(h)$ and $v_i^d(h)$ satisfy the following condition.

Lyapunov condition: There exists a parameter $\epsilon > 0$, such that the following equalities hold [31, p. 362].

$$\lim_{M \rightarrow \infty} \frac{1}{(\delta^{v,u}(h))^{2+\epsilon}} \sum_{i \in \mathcal{M}} \mathbb{E} \left[|v_i^u(h) - \mathbb{E} [v_i^u(h)]|^{2+\epsilon} \right] = 0, \quad (19)$$

$$\lim_{M \rightarrow \infty} \frac{1}{(\delta^{v,d}(h))^{2+\epsilon}} \sum_{i \in \mathcal{M}} \mathbb{E} \left[|v_i^d(h) - \mathbb{E} [v_i^d(h)]|^{2+\epsilon} \right] = 0, \quad (20)$$

where $\delta^{v,u}(h) = \sqrt{\sum_{i \in \mathcal{M}} (\delta_i^{v,u}(h))^2}$ and $\delta^{v,d}(h) = \sqrt{\sum_{i \in \mathcal{M}} (\delta_i^{v,d}(h))^2}$. Here, $\delta_i^{v,u}(h)$ and $\delta_i^{v,d}(h)$ are the standard deviations of $v_i^u(h)$ and $v_i^d(h)$, respectively. The values of $\delta_i^{v,u}(h)$ and $\delta_i^{v,d}(h)$ can be obtained based on the results of problem (18).

Next, we show that both $v_i^u(h)$ and $v_i^d(h)$ satisfy the Lyapunov condition. We introduce a parameter $F = \max_{i \in \mathcal{M}} (E_i^{\max} -$

Algorithm 1 Frequency regulation capacity scheduling algorithm executed by EV i before the operation hours

- 1: Initialize $\alpha, \eta, \mathcal{M}, \mathcal{H}, \mathcal{K}, \mathbb{E}[p^e(h)], \mathbb{E}[p^u(h)], \mathbb{E}[p^d(h)], \mathbb{E}[p^c(h)], h \in \mathcal{H}, f^{u,\max}, f^{d,\max}, \mu^u, \mu^d, E_i^{\max}, E_i^{\min}, s^{\max}, s^{\min}, p^b$, and l
 - 2: Generate scenarios $\omega_k, k \in \mathcal{K}$ based on historical records of the arrival and departure times of the EV
 - 3: Solve problem (18) to obtain $v_i^u(h, \omega_k), v_i^d(h, \omega_k)$, and $x_i(h, \omega_k), h \in \mathcal{H}$
 - 4: Send the values of $v_i^u(h, \omega_k), v_i^d(h, \omega_k)$, and $x_i(h, \omega_k), h \in \mathcal{H}, k \in \mathcal{K}$ to the aggregator
-

E_i^{\min}). F takes a finite value because the maximum hourly charged energy E_i^{\max} and minimum hourly charged energy E_i^{\min} of an EV $i \in \mathcal{M}$ are finite. We have $0 \leq v_i^u(h), v_i^d(h) \leq F$ based on (12b) and (12c). Then, we have

$$-F \leq v_i^u(h) - \mathbb{E}[v_i^u(h)], v_i^d(h) - \mathbb{E}[v_i^d(h)] \leq F. \quad (21)$$

According to [31, p. 362], since random variables $v_i^u(h)$ and $v_i^d(h)$ are bounded, c.f. (21), the Lyapunov condition is satisfied for both $v_i^u(h)$ and $v_i^d(h)$.

Let $\mathcal{N}(\mu, \delta^2)$ denote the normal distribution with mean μ and variance δ^2 . The aggregate regulation up capacity and regulation down capacity are modeled as normal distributions, which are given by

$$\sum_{i \in \mathcal{M}} v_i^u(h) \sim \mathcal{N}\left(\sum_{i \in \mathcal{M}} \mathbb{E}[v_i^u(h)], (\delta^{v,u}(h))^2\right), \quad (22)$$

$$\sum_{i \in \mathcal{M}} v_i^d(h) \sim \mathcal{N}\left(\sum_{i \in \mathcal{M}} \mathbb{E}[v_i^d(h)], (\delta^{v,d}(h))^2\right), \quad (23)$$

where $\mathbb{E}[v_i^u(h)] = \sum_{k \in \mathcal{K}} \mathcal{P}(\omega_k) v_i^u(h, \omega_k)$ and $\mathbb{E}[v_i^d(h)] = \sum_{k \in \mathcal{K}} \mathcal{P}(\omega_k) v_i^d(h, \omega_k)$. The values of $v_i^u(h, \omega_k)$ and $v_i^d(h, \omega_k)$ are obtained by solving problem (18).

The aggregator determines the capacities submitted in the DAM based on the distributions of $\sum_{i \in \mathcal{M}} v_i^u(h)$ and $\sum_{i \in \mathcal{M}} v_i^d(h)$. In particular, the values of the regulation up capacity $v^u(h)$ and regulation down capacity $v^d(h)$ submitted in the DAM are given by

$$v^u(h) = \sum_{i \in \mathcal{M}} \mathbb{E}[v_i^u(h)] - \Phi^{-1}(\beta) \delta^{v,u}(h), \quad (24)$$

$$v^d(h) = \sum_{i \in \mathcal{M}} \mathbb{E}[v_i^d(h)] - \Phi^{-1}(\beta) \delta^{v,d}(h), \quad (25)$$

where β is the desired confidence level (e.g., $\beta = 0.99$) and Φ^{-1} is the inverse of the cumulative distribution function of a standard normal distribution $\mathcal{N}(0, 1)$.

F. Algorithm and Implementation Issues

An algorithm for the EVs to schedule the frequency regulation capacity is presented in Algorithm 1. In the algorithm, the EV first initializes the parameters (Line 1). Then, the EV generates scenarios based on its historical arrival and departure times (Line 2). Subsequently, problem (18) is solved and the results are sent to the aggregator (Lines 3 – 4).

The implementation of the proposed algorithm requires an autonomous scheduler, a data collecting and storage system, a charging rate controller, and user interface. A block diagram

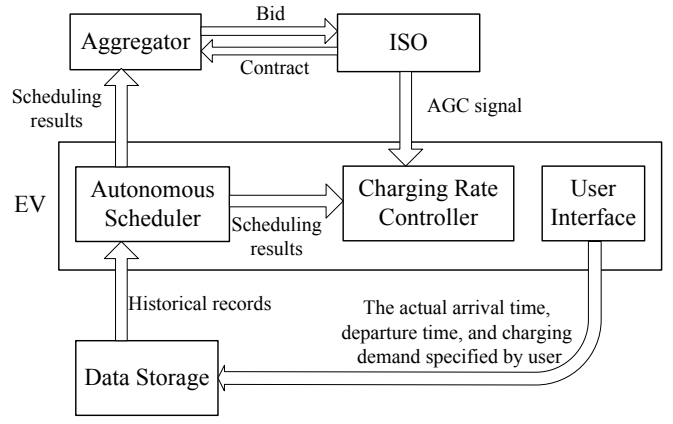


Fig. 4. A diagram of different components for the EV frequency regulation service.

for these components is shown in Fig. 4. The arrival and departure times of the EVs should be collected and stored in a database as records. These records can be used by an autonomous scheduler to generate scenarios for the proposed algorithm. On the day before the operation hours, the EVs schedule their capacity under different scenarios according to the proposed algorithm and send the results to an aggregator. The aggregator can generate a bid based on the EVs regulation capacity using (24) and (25). The bid will be submitted to the ISO in the market and the ISO will award a contract to allow the EVs to provide frequency regulation service. Then, during the operation hours on the next day, when an EV owner has parked the EV and plugged-in its charger, the user interface on the charger will be shown and encourage the EV owner to specify the departure time and charging demand requirement. If the EV owner skips this step, it means the departure time is unknown and the EV should be charged as fast as possible. Otherwise, if the EV owner specifies the departure time and charging demand requirement, these values are sent to the data storage. The arrival time is sent to the data storage without user intervention. Then, the EV generates a new scenario based on the actual value of the arrival time and the value of departure time specified by the user. Then, the EV runs the proposed algorithm with the new scenario and sends the results to the charging rate controller. The regulation capacity of an EV is uncertain because of the EV's random arrival and departure times. Equations (24) and (25) take into account the uncertainty of the regulation capacity and can be used to determine the values of the capacities submitted in the DAM. Finally, the aggregator retrieves the AGC signal from the ISO and controls the real-time charging rate of the EVs. When the AGC signal is positive in time slot t in hour h (i.e., $q(h, t) > 0$), the task of the aggregator is to decrease the charging rate of the EVs by $|q(h, t)|v^u(h)$. Otherwise, when $q(h, t) < 0$, the task is to increase the charging rate of the EVs by $|q(h, t)|v^d(h)$. The aggregator assigns the charging rates to the EVs according to the regulation capacity of each EV. In particular, each EV $i \in \mathcal{M}$ should adjust its charging rate to be $x_i(h) - \frac{v_i^u(h)|q(h, t)|v^u(h)}{\sum_{i \in \mathcal{M}} v_i^u(h)}$ or $x_i(h) + \frac{v_i^d(h)|q(h, t)|v^d(h)}{\sum_{i \in \mathcal{M}} v_i^d(h)}$, when $q(h, t)$ is positive or negative, respectively. In this manner, the aggregator provides exactly the amount of regulation capacity

submitted in the DAM.

Next, we discuss the advantages and limitations of the proposed approach compared to the existing literature [8]–[18]. The advantage of the proposed approach is that it takes into account the performance-based compensation scheme, which was not considered in [8]–[18]. On the other hand, since the proposed approach leverages the probabilistic robust optimization framework [27], which includes a heuristic parameter η to control the level of conservativeness, the limitation of the proposed approach is that it cannot guarantee that the EVs always follow the AGC signal. Instead, the proposed approach guarantees that the EVs follow the AGC signal with a certain probability, c.f. Section III-B.

IV. PERFORMANCE EVALUATION

In this section, we evaluate the performance of the proposed algorithm based on historical records of the AGC signal from PJM. We conducted a statistical analysis of the AGC signal data records [25] and obtained parameters $f^{u,\max} = 0.249$, $f^{d,\max} = 0.302$, $\mu^u = 0.134$, $\mu^d = 0.145$, $\lambda^u = 9.336$, and $\lambda^d = 8.585$. A sample of the AGC signal is shown in Fig. 5. The uncertainty of the AGC signal is taken into account in the proposed algorithm. We compare the proposed algorithm with a benchmark algorithm which has a deterministic formulation where the expected values of $f^u(h)$ and $f^d(h)$ are used in the formulation and uncertainty of the AGC signal is ignored. We compare with this benchmark algorithm to study the effect of the uncertain AGC signal on the EV frequency regulation service under the performance-based compensation scheme.

The prices of the performance-based compensation scheme from PJM [25] are used in the simulation. We averaged the regulation market capacity clearing price (RMCCP) and the regulation market performance clearing price (RMPCP) of PJM from Dec. 1, 2014 to Dec. 31, 2014. The average prices are shown in Fig. 6. The RMCCP (i.e., $p^u(h) + p^d(h)$) is the price of providing the frequency regulation capacity. The RMPCP (i.e., $p^c(h)$) is introduced under the performance-based compensation scheme to reimburse the market participants (e.g., EVs) for following the AGC signal. Note that the revenue for following the AGC signal is the product of RMPCP, the mileage of the AGC signal (i.e., $\lambda^u + \lambda^d$), and the capacity. On the other hand, the revenue of providing the capacity is the product of the RMCCP and the capacity. Hence, in Fig. 6, we present the price $p^c(h)(\lambda^u + \lambda^d)$ in order to compare with RMCCP fairly. As shown in Fig. 6, the price of following the AGC signal is significant for the performance-based compensation scheme and needs to be considered in the problem formulation and the simulations. Furthermore, we generate values of ξ_i using the following method to simulate the performance score in the performance-based compensation scheme. First, we test the algorithm outputs (i.e., $x_i(h, \omega_k)$, $v_i^u(h, \omega_k)$, $v_i^d(h, \omega_k)$) for the historical AGC signal from PJM. If EV i fails to follow the AGC signal in hour h under scenario ω_k , we have $\mathbf{1}_{i,h}(\omega_k) = 0$, where $\mathbf{1}_{i,h}(\omega_k)$ is the value of $\mathbf{1}_{i,h}$ in (6) under scenario ω_k . We denote $\mathcal{D}_{i,k}$ as the set of hours when $\mathbf{1}_{i,h}(\omega_k) = 0$ and $|\mathcal{D}_{i,k}|$ as its cardinality. As the performance score is based on the average performance of following the AGC signal in

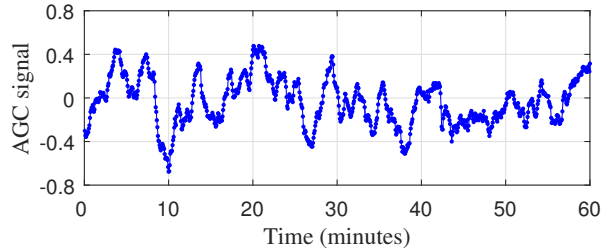


Fig. 5. A sample of the AGC signal in an hour obtained from PJM.

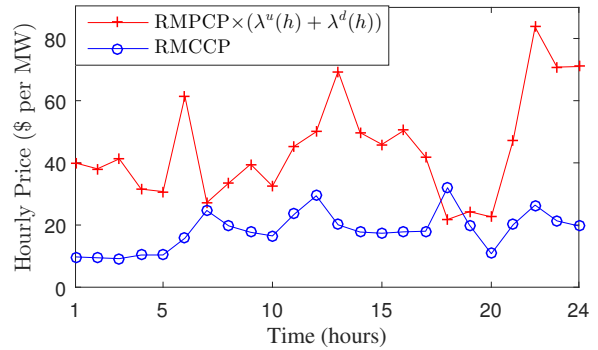


Fig. 6. The average hourly prices of frequency regulation service from PJM in Dec. 2014.

historical hours [24], we simulate the performance score by generating values as follows

$$\xi_i = 1 - \frac{\sum_{i \in \mathcal{M}} \sum_{k \in \mathcal{K}} |\mathcal{D}_{i,k}|}{MHK}.$$

We consider a fleet of 1000 EVs. The maximum charged energy in one hour is 10 kWh [32]. We first consider the case when the EVs have unidirectional chargers (charging only). The battery capacity of an EV is typically tens of kWh (e.g., 20 kWh for a Honda Fit and 85 kWh for a Tesla Model S). We assume a battery capacity of 40 kWh for simulation purpose. We consider an overnight charging case where EVs charge at night and are used for driving on the next day. The random arrival and departure times are generated according to [33] and there are 50 scenarios for each EV. The demand for charging energy is selected from [10, 30] kWh. We use $\beta = 0.99$ in (24) and (25) for simulation purpose.

In Fig. 7, we compare the proposed algorithm with the benchmark algorithm. As shown in Fig. 7, the proposed algorithm achieves a higher revenue than the benchmark algorithm under the performance-based compensation scheme. In particular, when the maximum hourly charged energy is 10 kWh, the average daily revenue increases from \$133 to \$151. This is because the proposed algorithm yields a solution which enables EVs to follow the AGC signal most of the time. On the other hand, with the benchmark algorithm where the uncertainty of the AGC signal is ignored, the EVs sometimes stop following the AGC signal when the EVs are fully charged. This will reduce the revenue under the performance-based compensation scheme. Additionally, as can be observed from Fig. 7, for both algorithms, the revenue increases as the maximum hourly charged energy increases. This is because the EVs can provide more regulation capacity when the chargers have higher charging power.

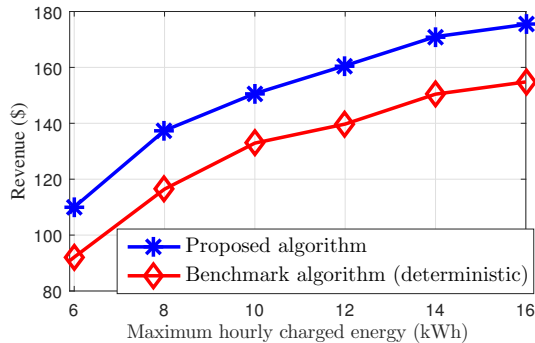


Fig. 7. Daily revenue versus the maximum hourly charged energy.

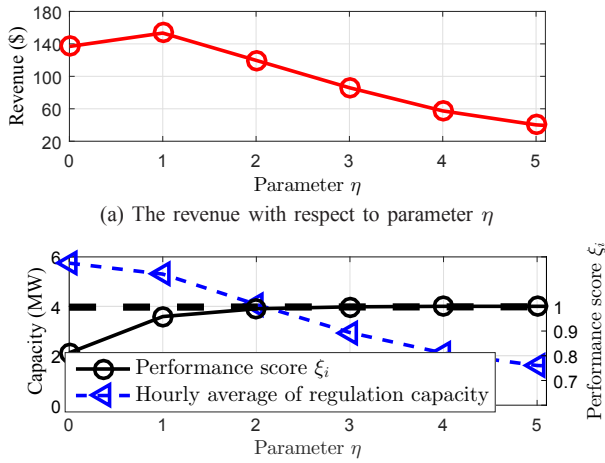


Fig. 8. (a) The revenue with respect to parameter η . (b) The regulation capacity and the performance score as a function of parameter η .

We study the effect of the tunable design parameter η on the proposed algorithm in Fig. 8. We first use the probability bounds in Section III-B to determine that $\eta \leq 5$ is needed, given that the EVs need to follow the AGC signal with a probability of 95%. The revenue as a function of parameter η is shown in Fig. 8(a). As can be observed from Fig. 8(a), when η increases, the revenue first increases when η is small and then decreases when η is large. This is because of the tradeoff between the regulation capacity and the performance score, which is shown in Fig. 8(b). As can be observed from Fig. 8(b), as η increases, the performance score increases while the regulation capacity decreases. Note that under the performance-based compensation scheme, the revenue depends on both the regulation capacity and the performance score for following the AGC signal. Based on the results in Fig. 8, parameter η is selected to be $\eta=1$ in this paper.

In Fig. 9, we show the probability that an EV follows the AGC signal. Thereby, we compare \mathcal{P}_i obtained via simulations with its lower bound obtained from (17). For an arbitrary EV i , we assume parameters $a_i = 1$ and $d_i = 13$. Fig. 9 confirms that the probability that an EV follows the AGC signal is not less than the right hand side of (17).

Next, we consider the situation when the EVs have bidirectional chargers which allow both charging and discharging. There is a battery degradation cost for the discharging. We assume the battery lasts for 800 life cycles, which is inferred

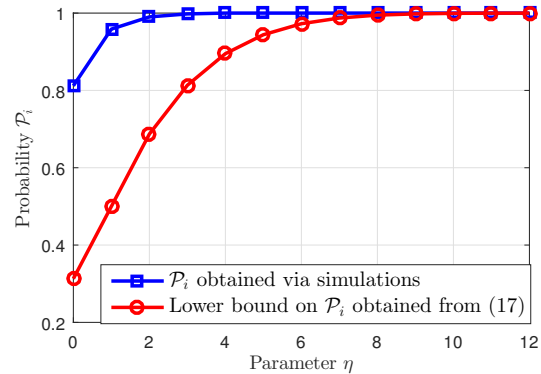


Fig. 9. Probability \mathcal{P}_i obtained via simulations and its lower bound obtained from (17).

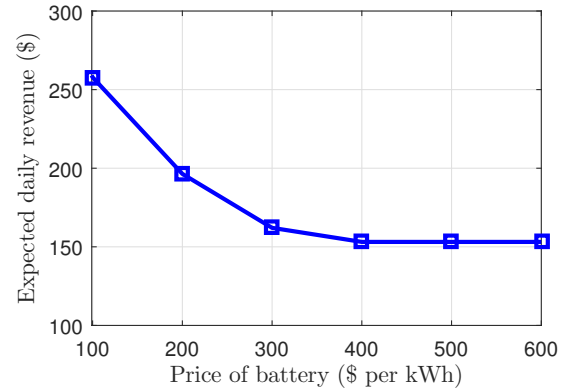


Fig. 10. Revenue as a function of the price of the battery. Note that we assumed a bidirectional charger in this figure.

from a battery limited warranty [34]. The battery degradation severity factor is obtained from [30] where the temperature is assumed to be 25 centigrade ($^{\circ}C$). According to [35], the prices of EV batteries have dropped from \$1000 per kWh to \$500 per kWh from year 2007 to year 2014. For the prices of \$500 per kWh, we found that the simulation results when the EVs have bidirectional chargers are actually similar to the results when the EVs use unidirectional chargers. This is because the battery degradation cost is taken into account in the objective function of our problem formulation. As the battery degradation cost is relatively high compared to the gain obtained from discharging, the solution obtained from the proposed algorithm will not instruct the EVs to discharge their batteries, if the price of the battery is \$500 per kWh. On the other hand, the prices of the battery are expected to drop further in the future. In Fig. 10, we present the expected daily revenue as a function of the price of the battery. Fig. 10 reveals that, the revenue of the frequency regulation service increases if the price of the battery can be decreased in the future. On the other hand, if the price of the battery is high, the EV batteries are not discharged for the frequency regulation service. As a result, the curve of the revenue becomes flat in Fig. 10 when the price of the battery is high.

V. CONCLUSION

In this paper, we studied the EV frequency regulation service under the performance-based compensation scheme. We first developed a model for the performance-based compen-

sation scheme by taking into account the market rules of the ISOs in the United States. Then, we formulated a problem to schedule the regulation capacity of the EVs and maximize the revenue under the performance-based compensation scheme. A robust optimization framework was used in the formulation to enable the EVs to follow the uncertain AGC signal most of the time. We performed numerical experiments using historical records of the AGC signal and prices from PJM. Simulation results showed that EVs can improve their revenue under the performance-based compensation scheme by taking into account the uncertainty of the AGC signal in their capacity scheduling. For future work, an interesting topic is to consider the scheduling of the EV regulation capacity when EVs are equipped with simple chargers which can only be turned on and off.

REFERENCES

- [1] W. Kempton, V. Udo, K. Huber, K. Komara, S. Letendre, S. Baker, D. Brunner, and N. Pearre, "A test of vehicle-to-grid (V2G) for energy storage and frequency regulation in the PJM system," Tech. Rep., Nov. 2008, available at: www.udel.edu/V2G/resources/test-v2g-in-pjm-jan09.pdf.
- [2] H. Ni, "PJM advanced technology pilots for system frequency control," in *Proc. of IEEE Innovative Smart Grid Technologies (ISGT)*, Washington, DC, Jan. 2012.
- [3] A. D. Papalexopoulos and P. E. Andrianesis, "Performance-based pricing of frequency regulation in electricity markets," *IEEE Trans. on Power Systems*, vol. 29, no. 1, pp. 441–449, Jan. 2014.
- [4] H. Liu, Z. Hu, Y. Song, and J. Lin, "Decentralized vehicle-to-grid control for primary frequency regulation considering charging demands," *IEEE Trans. on Power Systems*, vol. 28, no. 3, pp. 3480–3489, Aug. 2013.
- [5] Y. Ota, H. Taniguchi, T. Nakajima, K. M. Liyanage, J. Baba, and A. Yokohama, "Autonomous distributed V2G (vehicle-to-grid) satisfying scheduled charging," *IEEE Trans. on Smart Grid*, vol. 3, no. 1, pp. 559–564, Mar. 2012.
- [6] T. Masuta and A. Yokoyama, "Supplementary load frequency control by use of a number of both electric vehicles and heat pump water heaters," *IEEE Trans. on Smart Grid*, vol. 3, no. 3, pp. 1253–1262, Sept. 2012.
- [7] H. Yang, C. Y. Chung, and J. Zhao, "Application of plug-in electric vehicles to frequency regulation based on distributed signal acquisition via limited communication," *IEEE Trans. on Power Systems*, vol. 28, no. 2, pp. 1017–1026, May 2013.
- [8] E. Sortomme and K. W. Cheung, "Intelligent dispatch of electric vehicles performing vehicle-to-grid regulation," in *Proc. of IEEE International Electric Vehicle Conf. (IEVC)*, Greenville, SC, Mar. 2012.
- [9] J. Lin, K.-C. Leung, and V. O. K. Li, "Online scheduling for vehicle-to-grid regulation service," in *Proc. of IEEE SmartGridComm*, Vancouver, Canada, Oct. 2013.
- [10] S. Sun, M. Dong, and B. Liang, "Real-time welfare-maximizing regulation allocation in dynamic aggregator-EVs system," *IEEE Trans. on Smart Grid*, vol. 5, no. 3, pp. 1397–1409, May 2014.
- [11] C. Wu, H. Mohsenian-Rad, and J. Huang, "Vehicle-to-aggregator interaction game," *IEEE Trans. on Smart Grid*, vol. 3, no. 1, pp. 434–442, Mar. 2012.
- [12] S. Han, S. Han, and K. Sezaki, "Development of an optimal vehicle-to-grid aggregator for frequency regulation," *IEEE Trans. on Smart Grid*, vol. 1, no. 1, pp. 65–72, June 2010.
- [13] E. Sortomme and M. El-Sharkawi, "Optimal charging strategies for unidirectional vehicle-to-grid," *IEEE Trans. on Smart Grid*, vol. 2, no. 1, pp. 131–138, Mar. 2011.
- [14] C. Jin, J. Tang, and P. Ghosh, "Optimizing electric vehicle charging with energy storage in the electricity market," *IEEE Trans. on Smart Grid*, vol. 4, no. 1, pp. 311–320, Mar. 2013.
- [15] J. Donadee and M. D. Ilic, "Stochastic optimization of grid to vehicle frequency regulation capacity bids," *IEEE Trans. on Smart Grid*, vol. 5, no. 2, pp. 1061–1069, Mar. 2014.
- [16] —, "Stochastic co-optimization of charging and frequency regulation by electric vehicles," in *Proc. of IEEE North American Power Symposium (NAPS)*, Champaign, IL, Jan. 2012.
- [17] S. I. Vagropoulos and A. G. Bakirtzis, "Optimal bidding strategy for electric vehicle aggregators in electricity markets," *IEEE Trans. on Power System*, vol. 28, no. 4, pp. 4031–4041, Nov. 2013.
- [18] S. I. Vagropoulos, D. K. Kyriazidis, and A. G. Bakirtzis, "Real-time charging management framework for electric vehicle aggregators in a market environment," accepted for publication in *IEEE Trans. on Smart Grid*, 2015.
- [19] E. Yao, V.W.S. Wong, and R. Schober, "A robust design of electric vehicle frequency regulation service," in *Proc. of IEEE SmartGridComm*, Venice, Italy, Nov. 2014.
- [20] FERC Order 755: Frequency Regulation Compensation in the Organized Wholesale Power Markets, Oct. 2011, Available at: <http://www.ferc.gov/whats-new/comm-meet/2011/102011/E-28.pdf>, accessed Jan. 2016.
- [21] C. Quinn, D. Zimmerle, and T. H. Bradley, "An evaluation of state-of-charge limitations and actuation signal energy content on plug-in hybrid electric vehicle, vehicle-to-grid reliability, and economics," *IEEE Trans. on Smart Grid*, vol. 3, no. 1, pp. 483–491, Mar. 2012.
- [22] C. Quinn, "Evaluation of distributed energy storage for ancillary service provision," Master's thesis, Colorado State University, 2011.
- [23] California ISO (CAISO) Business Practice Manual for Market Operations, Version 45, Nov. 2015, Available at: <https://bpmcm.caiso.com/Pages/BPMDetails.aspx?BPM=Market%20Operations>, accessed Jan. 2016.
- [24] PJM Manual 11: Energy and Ancillary Services Market Operations, Revision 79, Dec. 2015, Available at: <http://www.pjm.com/~media/documents/manuals/m11.ashx>.
- [25] PJM Frequency Regulation Market Historical Records of Prices and AGC Signals, Available at: <http://www.pjm.com/markets-and-operations/ancillary-services.aspx>, accessed Sept. 2015.
- [26] SAE J1772 Standard on Electric Vehicle and Plug-in Hybrid Electric Vehicle Conductive Charge Coupler, Available at: http://standards.sae.org/j1772_201001/, accessed Sept. 2015.
- [27] D. Bertsimas and M. Sim, "The price of robustness," *Operations Research*, vol. 52, no. 1, pp. 35–53, Feb. 2004.
- [28] A. Ben-Tal and A. Nemirovski, "Robust optimization methodology and applications," *Mathematical Programming*, vol. 92, no. 3, pp. 453–480, May 2002.
- [29] J. Donadee and M. D. Ilic, "Estimating the rate of battery degradation under a stationary Markov operating policy," in *Proc. of IEEE PES General Meeting*, National Harbor, MD, Jul. 2014.
- [30] S. Onori, P. Spagnol, V. Marano, Y. Guezennec, and G. Rizzoni, "A new life estimation method for Lithium-ion batteries in plug-in hybrid electric vehicles applications," *Intl. J. of Power Electronics*, vol. 4, no. 3, pp. 302–319, June 2012.
- [31] P. Billingsley, *Probability and Measure, Third Ed.* John Wiley and Sons, 1995.
- [32] Tesla Motor outlet charging adapter guide, Available at: https://www.teslamotors.com/en_CA/models-charging#/basics, accessed Jan. 2016.
- [33] A. Santos, N. Meguckin, H. Nakamoto, D. Gray, and S. Liss, "Summary of travel trends: 2009 National household travel survey," U.S. Department of Transportation, Federal Highway Administration, Tech. Rep., June 2011, Available at: <http://nhts.ornl.gov/2009/pub/stt.pdf>.
- [34] Tesla Motors model S vehicle warranty, Available at: https://www.teslamotors.com/sites/default/files/blog_attachments/ms_vehicle_warranty.pdf, accessed Aug. 2015.
- [35] B. Nykvist and M. Nilsson, "Rapid falling costs of battery packs for electric vehicles," *Nature Climate Change*, vol. 5, no. 4, pp. 329–332, Apr. 2015.



Enxin Yao (S'11) received the B.S. and the M.S. degrees from Peking University, Beijing, China in 2008 and 2011, respectively. He is currently a Ph.D. candidate in the Department of Electrical and Computer Engineering, the University of British Columbia, Vancouver, Canada. He is interested in the area of the smart grid. His current research focus on demand side management and electric vehicle frequency regulation service.



Vincent W.S. Wong (S'94, M'00, SM'07, F'16) received the B.Sc. degree from the University of Manitoba, Winnipeg, MB, Canada, in 1994, the M.A.Sc. degree from the University of Waterloo, Waterloo, ON, Canada, in 1996, and the Ph.D. degree from the University of British Columbia (UBC), Vancouver, BC, Canada, in 2000. From 2000 to 2001, he worked as a systems engineer at PMC-Sierra Inc. He joined the Department of Electrical and Computer Engineering at UBC in 2002 and is currently a Professor. His research areas include

protocol design, optimization, and resource management of communication networks, with applications to wireless networks, smart grid, and the Internet. Dr. Wong is an Editor of the *IEEE Transactions on Communications*. He is a Guest Editor of *IEEE Journal on Selected Areas in Communications*, special issue on "Emerging Technologies" in 2016. He has served on the editorial boards of *IEEE Transactions on Vehicular Technology* and *Journal of Communications and Networks*. He has served as a Technical Program Co-chair of *IEEE SmartGridComm'14*, as well as a Symposium Co-chair of *IEEE SmartGridComm'13* and *IEEE Globecom'13*. He is the Chair of the IEEE Communications Society Emerging Technical Sub-Committee on Smart Grid Communications and the IEEE Vancouver Joint Communications Chapter. He received the 2014 UBC Killam Faculty Research Fellowship.



Robert Schober (S'98, M'01, SM'08, F'10) was born in Neuendettelsau, Germany, in 1971. He received the Diplom (Univ.) and the Ph.D. degrees in electrical engineering from the University of Erlangen-Nuernberg in 1997 and 2000, respectively. From May 2001 to April 2002 he was a Postdoctoral Fellow at the University of Toronto, Canada, sponsored by the German Academic Exchange Service (DAAD). Since May 2002 he has been with the University of British Columbia (UBC), Vancouver, Canada, where he is now a Full Professor. Since

January 2012 he is an Alexander von Humboldt Professor and the Chair for Digital Communication at the Friedrich Alexander University (FAU), Erlangen, Germany. His research interests fall into the broad areas of Communication Theory, Wireless Communications, and Statistical Signal Processing.

Dr. Schober received several awards for his work including the 2002 Heinz MaierLeibnitz Award of the German Science Foundation (DFG), the 2004 Innovations Award of the Vodafone Foundation for Research in Mobile Communications, the 2006 UBC Killam Research Prize, the 2007 Wilhelm Friedrich Bessel Research Award of the Alexander von Humboldt Foundation, the 2008 Charles McDowell Award for Excellence in Research from UBC, a 2011 Alexander von Humboldt Professorship, and a 2012 NSERC E.W.R. Steacie Fellowship. In addition, he received best paper awards from the German Information Technology Society (ITG), the European Association for Signal, Speech and Image Processing (EURASIP), *IEEE WCNC 2012*, *IEEE Globecom 2011*, *IEEE ICUWB 2006*, the *International Zurich Seminar on Broadband Communications*, and *European Wireless 2000*. Dr. Schober is a Fellow of the Canadian Academy of Engineering and a Fellow of the Engineering Institute of Canada. From 2012 to 2015, he was the Editor-in-Chief of the *IEEE Transactions on Communications*. He currently serves as a Member-at-Large on the Board of Governors of the IEEE Communication Society and as Chair of the Steering Committee of the *IEEE Transactions on Molecular, Biological and Multiscale Communications*.